Available online at www.sciencedirect.com

ScienceDirect

Ceramics International 40 (2014) 951–960

CERAMICS INTERNATIONAL

www.elsevier.com/locate/ceramint

Microstructure and compressibility of SiC nanoparticles reinforced Cu nanocomposite powders processed by high energy mechanical milling

M.R. Akbarpour[a,*], E. Salahi[b], F. Alikhani Hesari[b], A. Simchi[c], H.S. Kim[d]

[a]Division of Materials Engineering, Department of Engineering, University of Maragheh, Maragheh, East Azerbaijan, Iran
[b]Materials and Energy Research Center (MERC), P.O. Box 14155-4777, Tehran, Iran
[c]Department of Materials Science and Engineering and Institute for Nanoscience and Nanotechnology, Sharif University of Technology, P.O. Box 11365-9466, Tehran, Iran
[d]Department of Materials Science and Engineering, Pohang University of Science and Technology, Pohang 790-784, South Korea

Received 16 April 2013; received in revised form 21 June 2013; accepted 24 June 2013
Available online 1 July 2013

Abstract

Cu/SiC nanocomposite powders with homogeneously distributed nanosize SiC particles were produced by high energy mechanical milling (MM). Scanning electron microscopy, transmission electron microscopy, X-ray diffraction, and micro-hardness and density measurements were performed to understand the effects of microstructure and hardness on compaction behavior during MM. The effects of SiC nanoparticle content and mechanical milling time on apparent density (AD) and tap density (TD) of the nanocomposite powders were systematically investigated. The Hausner ratio (HR), defined as TD to AD, were estimated to evaluate friction between the particles. Increasing MM duration and SiC content resulted in a decrease in HR due to the changes in morphology and hardness of the powders. Additionally, the compressibility behavior of the powders was theoretically examined using a compaction equation to investigate the deformation capacity. Densification parameters of the nanocomposite powders showed a significant decrease with increasing MM duration and a slight decrease with increasing SiC content.

Keywords: Nanocomposite powder; Copper; SiC nanoparticles; Compressibility; Microstructure

1. Introduction

Cu/SiC metal matrix composites (MMCs) have been the subject of extensive research due to their excellent electrical and thermal conductivities, enhanced hardness, good wear resistance, and frictional properties [1–3]. These composites already have many applications in the fields of welding electrodes and electrical contacts [4]. Generally, the first requirement for the particle reinforced composite materials to show their superior performance is homogeneous distribution of the reinforcing phases [5].

Agglomeration of reinforcement particles deteriorates mechanical properties of MMCs. Differences in particle size, densities, geometries, flowing or the development of an electrical charge contribute to particle agglomeration [6]. In powder metallurgy, the matrix and reinforcement mixing process is a critical step towards a homogeneous distribution throughout the consolidated composite materials [7,8]. One of the methods to improve particle distribution is using mechanical milling (MM) technique which has capability to incorporate reinforcement particles into the metal matrix in a close distance [9–11]. The major mechanism responsible for structuring such kind of microstructures is repeated fracturing and cold welding of particles due to collisions of the powders with balls media [12]. However, the MM process generally brings some disadvantages that (i) cold worked structure decreases the compressibility of powders and (ii) the contamination of the powders by gaseous elements affects the integrity of densification during sintering [13–16].

Up to now, studies of Cu reinforced with nanosize SiC (n-SiC) prepared by MM has seldom been reported. Compaction

*Corresponding author. Tel.: +98 2636280040; fax: +98 2188773352.
E-mail address: mreza.akbarpour@gmail.com (M.R. Akbarpour).

0272-8842/$ - see front matter © 2013 Elsevier Ltd and Techna Group S.r.l. All rights reserved.
http://dx.doi.org/10.1016/j.ceramint.2013.06.091

in powder metallurgy is of interest in MM processed composites. Also, there is only limited information concerning the properties and densification of the MM processed Cu/SiC nanocomposite in the literature. It should be noted that n-SiC is a promising reinforcement material for Cu due to its low price, high hardness, good resistance to wear, and good corrosion resistance. Therefore, in this study, Cu-based composites reinforced with different volume fractions of n-SiC were produced by MM with different processing times. The effects of MM time and n-SiC on powder morphology, friction between particles, and compressibility of the MM processed powders were investigated, especially in terms of the densification parameter (A) of the Panelli–Ambrosio Filho equation [17].

2. Experimental

Cu (99.7% purity and $< 20\,\mu m$ size range supplied from Merck Co., Germany) and n-SiC particles (+99% purity, approximately 40 nm in diameter, Nabond Co.) were used in this study. The starting materials were characterized by scanning electron microscopy (SEM, Philips XL30). Fig. 1(a) and (b) shows SEM micrographs of the starting materials. Four compositions were used: 0, 2, 4, and 6 vol% SiC with the balance of Cu. Powder mixtures of each composition were placed in a stainless steel mixing jar containing stainless steel milling balls of 10 mm diameter with an initial ball-to-powder weight ratio (BPR)= 10:1. The jars were filled with argon and then agitated with a planetary ball mill at 300 rpm for 25 h. The Fe contamination of the powders during mechanical milling was traced by using inductively coupled plasma (ICP) mass spectrometry.

The samples were taken from each batch at regular intervals for microstructural and morphological analyses. The ball milled powders were examined using SEM in order to characterize the particle morphology and size. A tranmission electron microscope (TEM, FEG Philips CM 200) was used to study the dispersion of the n-SiC particles within the Cu matrix. The grain size of Cu matrix after MM were determined by X-ray diffraction (XRD) using a D8 Advance Bruker diffractometer with CuKα radiation ($\lambda = 0.154$ nm) by the step size of 0.02°. The grain size was calculated by Williamson–Hall's method considering the instrumental broadening effect [18].

The Vickers microhardness test was carried out using an Olympus microhardness tester (FM-700) with a load of 50 g for 10 s. The powder samples for microhardness test were mounted in a conductive polymer and polished with a final polishing step using 0.05 μm colloidal diamond. At least 20 measurements were made on each sample (on the particles located on the polished surface).

The MM processed powders were characterized by their morphology (i.e. shape), apparent density (AD), and tap density (TD). The particle size of the powders was measured using a laser scattering technique. The AD or random loose packing of the powders was determined by the standard (ISO 3923) cup and funnel method, and the TD or random dense packing of the powders was measured by a tap density tester.

The MM processed powders were consolidated using cold uniaxial pressing in a cylindrical rigid die at 200, 400, 600, and 800 MPa with zinc stearate as a die lubricant. The compacted samples of 10 mm diameter and approximately 5 mm thick pellets were obtained, which were used to determine the compressibility curves of the powders. The density of the compacts was estimated precisely by the Archimedes method. The estimated error in the density measurements was less than 1.5%. The results were averaged over two independent measurements.

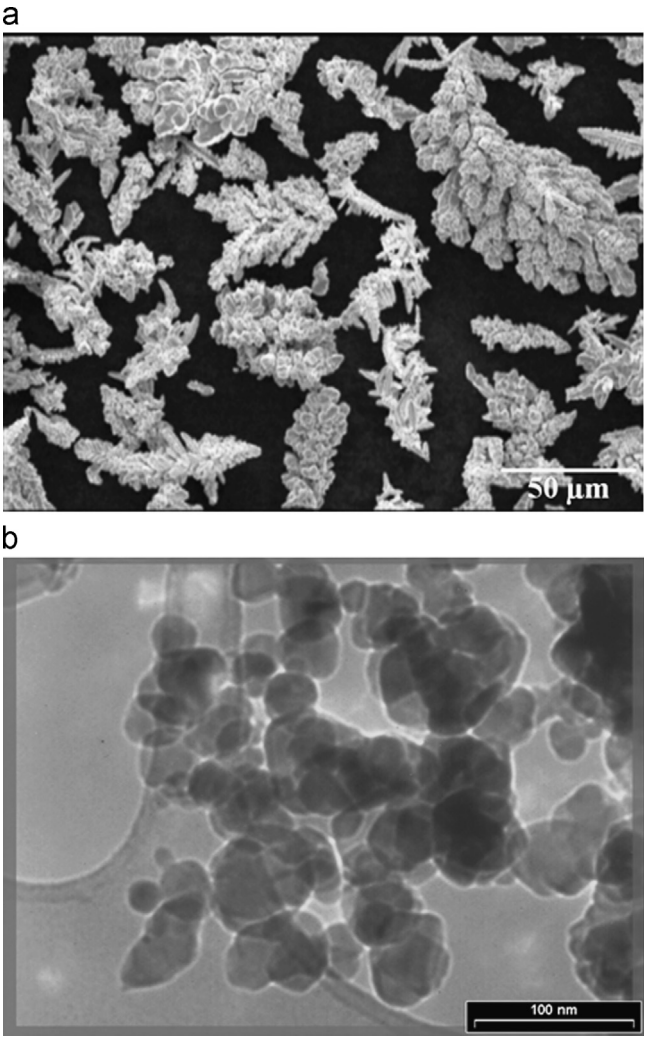

Fig. 1. (a) SEM micrograph of Cu powder and (b) TEM micrograph of n-SiC particles.

3. Results and discussion

3.1. Powders morphology

Fig. 2(a)–(e) shows the morphological variations for Cu/4 vol% SiC powder during MM up to 25 h. During high-energy MM, the powder particles are repeatedly flattened, cold welded, fractured, and rewelded. Plastic deformation and cold welding are predominant during initial MM, in which the deformation leads to a change in particle shape, and cold welding leads to an increase in particle size and the formation of layered structures [19]. After 1 h MM, the electrolytic Cu powder (Fig. 1(a)) was flattened (Fig. 2(a)) due to the impact forces exerted on the powder by the steel balls and

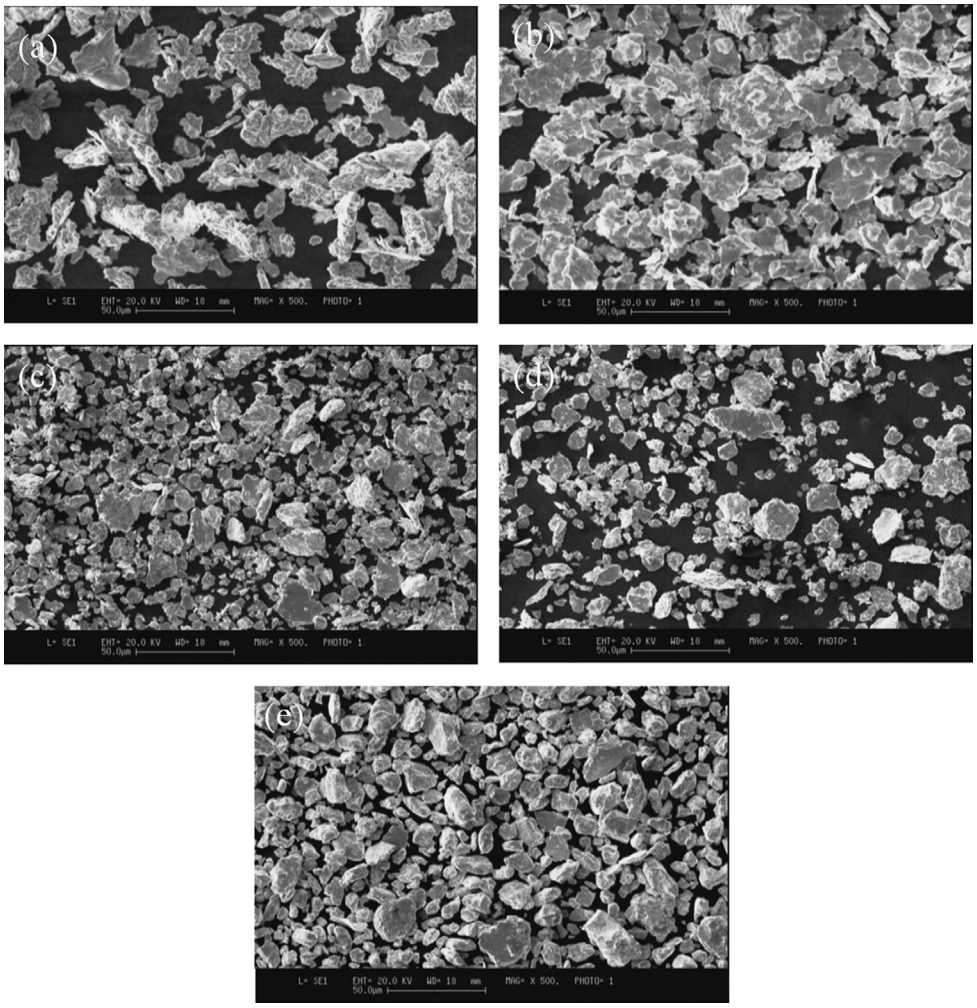

Fig. 2. Morphology of the Cu/4 vol% SiC composite powder after mechanical milling times of (a) 1 h and (b) 5 h, particle flattening, (c) 10 h, welding predominance, (d) 15 h, equiaxed particle formation (fracturing dominance) and (e) 25 h, semi-equiaxed particles.

welded with increasing time up to 5 h (Fig. 2(b)). With increasing milling time, the powder shape transformed from flattened to equiaxed, and the particle size increased to approximately 30 μm (Fig. 2(c)). The predominant mechanism at this stage was plastic deformation and cold welding. As the mechanical milling process is prolonged, the ability of the particles to accept further plastic deformation is diminished. Therefore, the fracturing became a significant process and resulted in a decrease in the particle size until the equilibrium between cold welding and fracturing occurred (Fig. 2(d) and (e)). The microstructural evolution during the high-energy MM process observed for the Cu reinforced with n-SiC which is in good agreement with the model of Lu et al. [10] presenting a scheme of the evolution of distribution of the SiC particles in the aluminum matrix during MM.

As shown in Fig. 2, the particle size increases during the first stage and then decreases with increasing MM time. It is clear that heavy deformation is introduced into the particles during MM. This is manifested by the presence of a variety of crystal defects such as dislocations, vacancies, stacking faults, and increased number of grain boundaries. The effect of milling time on the powder morphology of composite powders has been studied separately by Adamiak [20] and Gan and Gu [21]. A similar trend has been observed in all cases.

The morphology of 10 h MM processed Cu powders with different volume fractions of the n-SiC is shown in Fig. 3. According to the figure, the pure Cu includes large particles with completely flat shape. It is observed that with increasing the volume fraction of n-SiC, finer composite powders with more uniform particle size distribution are obtained. The morphology of the particles reaches steady state at shorter milling times due to the effect of n-SiC during accelerated MM (welding and fracturing) through an additional deformation on the matrix [22].

3.2. Powder microstructure

The XRD patterns for Cu/4 vol% SiC powder at different MM times are shown in Fig. 4, revealing the structural evolution of the powder mixture as the milling process progressed. Dependence of deformation behavior in the powder during different stages of MM can be evaluated by the change in diffraction intensity ratios for four major peaks in Cu/4 vol% SiC powder. The results did not show any preferential deformation direction. The XRD peaks were

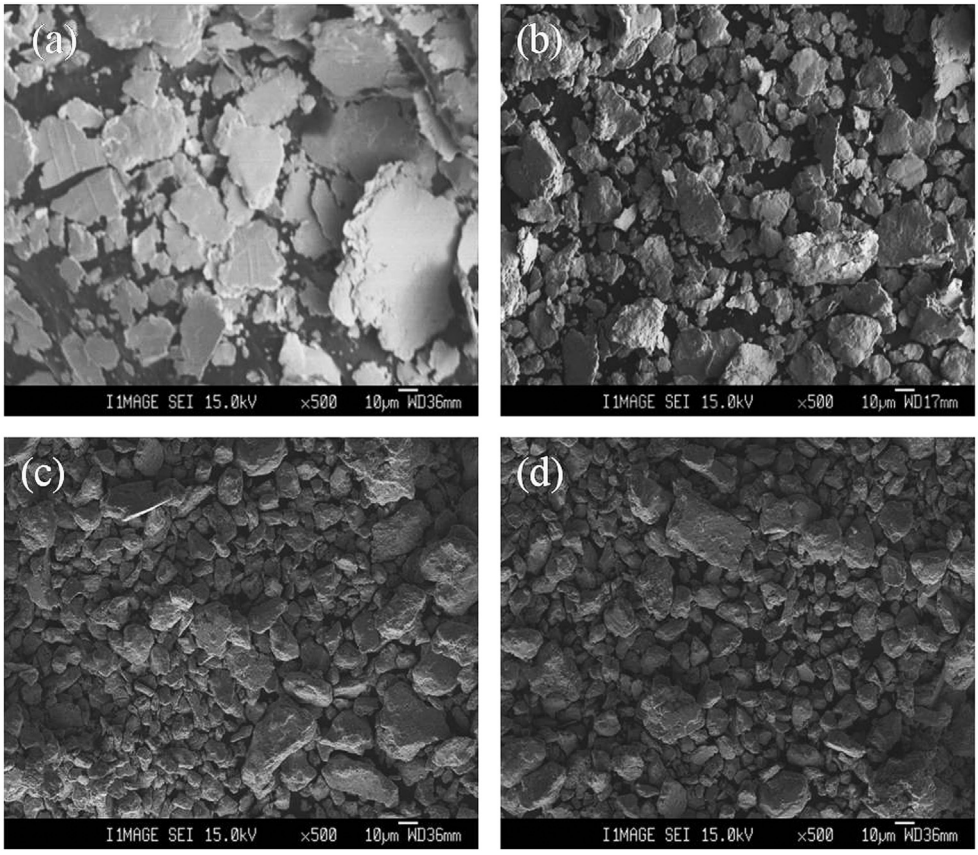

Fig. 3. Morphology of the Cu/*x*SiC composite powders processed by MM for 10 h: (a) Cu, (b) Cu-2 vol% SiC, (c) Cu-4 vol% SiC and (d) Cu-6 vol% SiC.

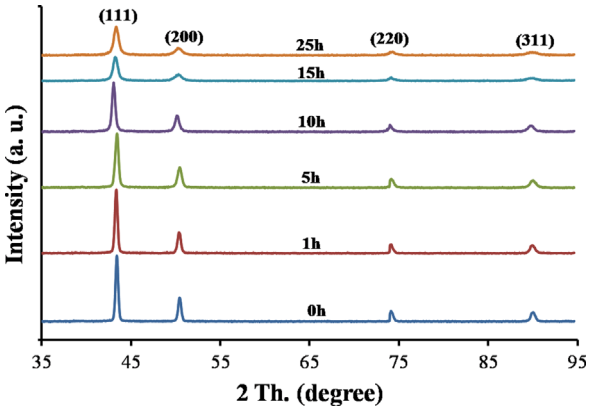

Fig. 4. XRD patterns of the Cu/4 vol% SiC powder milled for 0, 1, 5, 10, 15, and 25 h.

broadened, and their intensities were decreased with increasing milling time. The peak broadening detected in the patterns suggests that both the grain size of the powders and the change in lattice distortion are significantly affected by MM. Fig. 5 shows the variation of grain size calculated from the Williamson–Hall plots [18] and Vickers microhardness of the MM processed powders for different milling time. Grain size decreased with increasing milling time then reached a minimum at the steady state condition. Also, it was seen that the crystallite size decreased rapidly at the initial stage of milling as milling time increased, and it reached steady state in a shorter time, which is in agreement with the previous results [23]. According to Fig. 5, the hardness of the mechanically milled powders increased with decreasing of the grain size. Increasing the hardness of the nanocomposite powders affected the deformation capability during compaction which will be shown in the next section. Fig. 6(a) shows the bright field TEM micrograph of Cu/4 vol% SiC powder mechanically milled for 25 h, in which the SiC nanoparticles have been dispersed in the nanocrystalline Cu matrix. Also, dark field TEM micrograph of Fig. 6(a) is shown in (b), indicating the homogeneous dispersion of second phase in the matrix. Analysis of the bright parts (part no.1) in Fig. 6(b) is given in Fig. 6(c), which corresponds to the composition of SiC nanoparticle. Also, there are some elongated grains in the microstructure (part 2 in Fig. 6(a)) which contain Fe in the composition (Fig. 6(d)), indicating contamination of the powder by Fe during the mechanical milling process. The content of the contamination for Cu/4 vol% SiC nanocomposite measured about 0.2 wt% by ICP mass spectrometry.

3.3. Apparent density, tap density and Hausner ratio

Fig. 7(a) shows the dependence of AD and TD as a function of MM time for the Cu reinforced with 4 vol% SiC powder. A similar trend for AD and TD is seen with increasing MM time. The density continuously decreases during the initial stage of milling, and it reaches a minimum value (up to 5 h) and then starts to increase with prolonging milling time. These results are in agreement with the other reports [22]. The reason

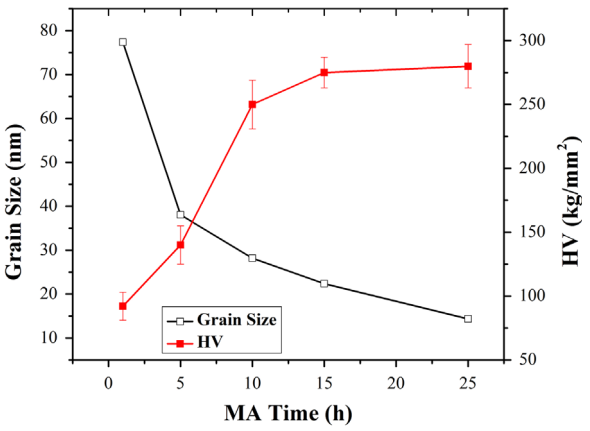

Fig. 5. Grain size and Vickers micro-hardness of Cu/4 vol% SiC composites vs. MM time.

for a decrease in density at the first stage of MM is high friction and formation of bridges between particles due to the formation of large and flake like particles (as shown in Fig. 2) and an increase in the particle size [16]. Irregularity of the powders hinders the particles mobility and their ability to attain better configuration. In the case of flattened particles, they can bridge gap between particles and create large voids. The ratio of TD to AD of a powder mass is termed Hausner Ratio [24]. The values of this ratio measure the relative magnitude of the friction between the particles in that mass. Variation of the Hausner Ratio with increasing MA time is shown in Fig. 7(b). The Hausner ratio decreases from 1.097 to 1.0133 during MM, which demonstrates the decrease of cohesivity of the powders with increasing work hardening. Therefore, the friction between the nanocomposite powders decreases with increasing MM time. The mixed powder microstructure including the Cu and agglomerates of n-SiC shows high friction between the particles. The main decrease in this ratio happens during MM time of 5–10 h, which corresponds to the morphological change of the powder from flaky shape to equiaxed shape and severe increase in work hardening. After MM for 15 h, slight decrease in HR due to MM is seen. At this stage the main phenomenon is the decrement of the particle size.

The effect of SiC vol% on TD and AD after MM for 25 h is shown in Fig. 8(a). According to Fig. 8(a), TD and AD increase with the addition of n-SiC. It is related to the particle size and fraction of powders with irregular morphology. Higher amount of SiC particles results in more equiaxed particles of smaller sizes. Fig. 8(b) shows the decrease of the Hausner ratio with the addition of SiC. The distribution of the particle size in the pure Cu and Cu reinforced with 4 vol% SiC after MM for 25 h is shown in Fig. 9. The decrease of the particle size due to the n-SiC addition is obvious. Addition of the 4 vol% SiC results in the decrease of D_{50} from 41.22 μm to 21.39 μm. The brittle n-SiC particles tend to become occluded by the ductile constituents and trapped inside the Cu particles during the welding stage. The presence of the reinforcement particles between the Cu particles increases local deformation in the vicinity of the reinforcement particles, thus high deformation of the Cu matrix develops around the reinforcement particle. The improvement in the welding and fracture mechanisms due to the presence of n-SiC particles causes the

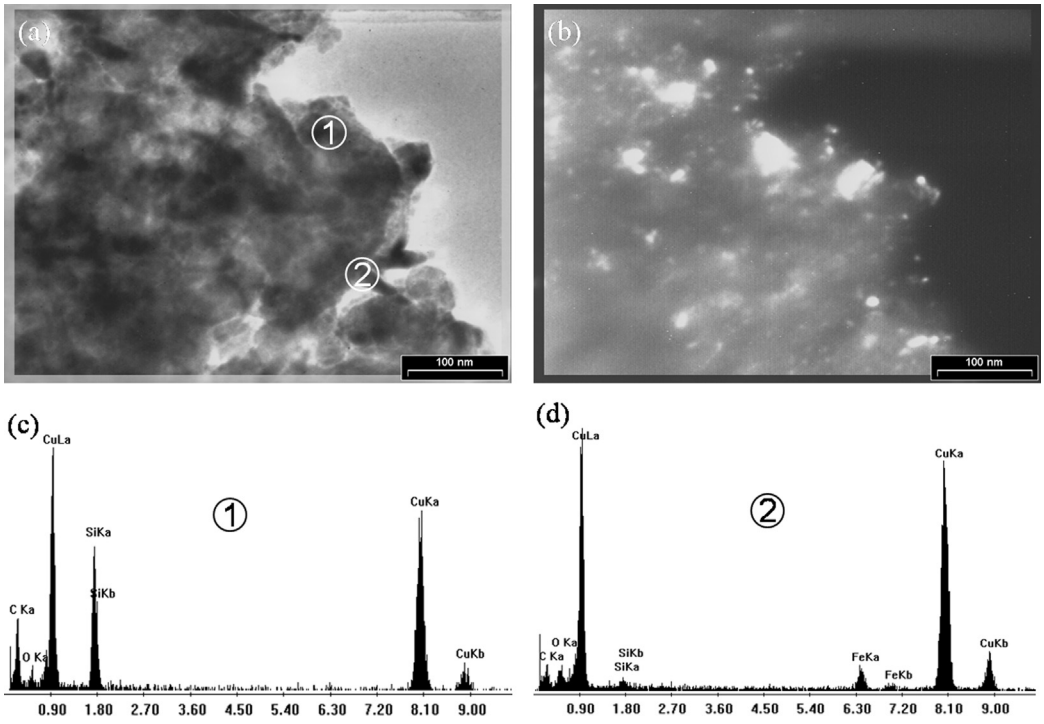

Fig. 6. (a and b) Bright field and dark field TEM micrographs of Cu/4 vol% SiC powder mechanically milled for 25 h, (c) chemical analysis of the part no.1 in section corresponding to the Cu/SiC composition (a) and (d) chemical analysis of the part no.2 in section (a), indicating contamination of the powder by Fe during the mechanical milling process.

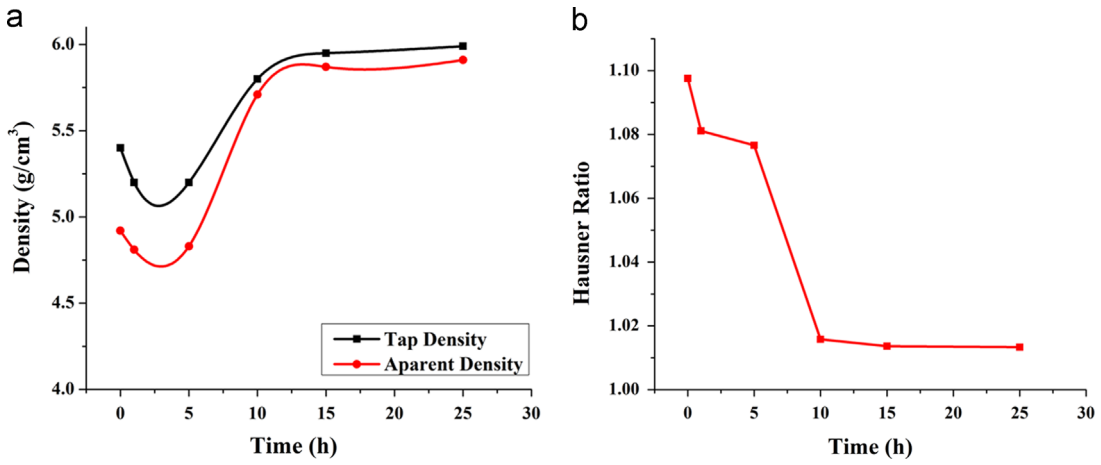

Fig. 7. (a) TD and AD vs. MM time and (b) HR vs. MM time for Cu/4 vol% SiC nanocomposite.

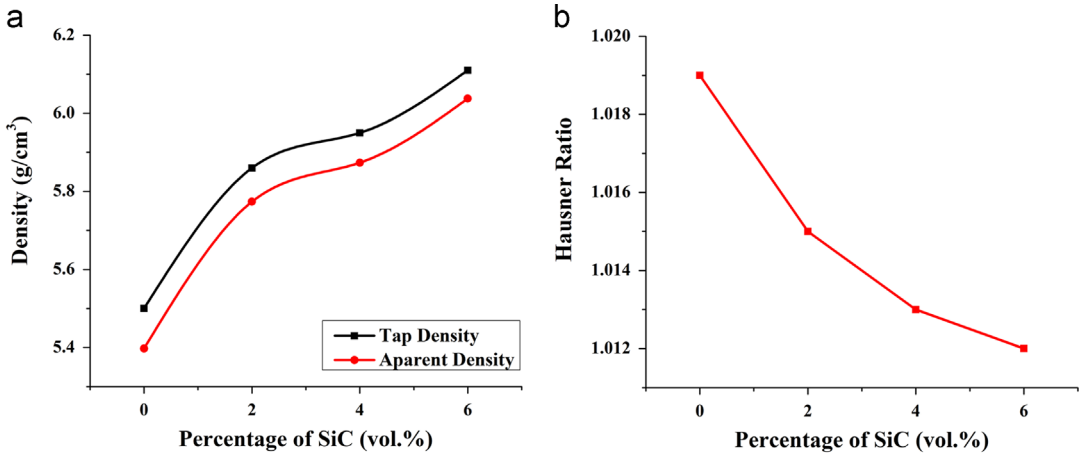

Fig. 8. (a) TD and AD vs. n-SiC vol% and (b) HR vs. n-SiC vol% mechanically milled for 25 h.

MM process to be completed in a shorter time. Therefore, a smaller average particle size in the nanocomposite powder with higher SiC content can be obtained.

3.4. Compressibility of Cu/x vol% SiC composite powder

Powder compaction is conventionally divided into several stages and each stage is considered to be interrelated in terms of the physical and mechanical properties of the powder particles [25]. The initial stage of compaction involves particle rearrangement; this stage is largely affected by the physical (spatial) properties of particles such as particle size and shape. In the second stage, it is considered that elastic and plastic deformations take place and the mechanical properties and purity of particles become dominant factors. The final stage is almost entirely due to cold working of the bulk material and is affected by the deformation and work hardening of particles. However, due to differences in density and stress distributions, there may be an overlap of the different stages during the consolidation process. This is caused by frictional forces in-between particles and/or particles and the die wall [22].

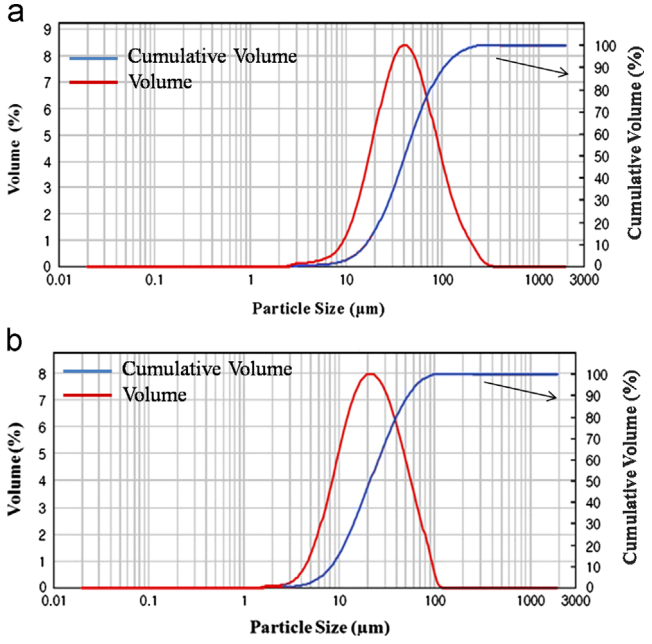

Fig. 9. Particle/agglomerate size distributions of the MA processed powders for 25 h: (a) Cu and (b) Cu/4 vol%SiC nanocomposite.

Fig. 10 shows the relative density of the blended Cu/4 vol% SiC powder and mechanical milled Cu/4 vol% SiC for different MM times as a function of applied pressure. In general, the curves indicate the typical powder compressibility behavior of metallic powders, i.e. the density increases with increasing compaction pressure at a decelerating rate. The blended powders including the Cu powder with dendritic morphology and high level of deformation capability (low hardness value), and the n-SiC agglomerates showed better compressibility behavior than the mechanically milled powders. The blended Cu/4 vol% SiC powder could reach ~95% of theoretical density at high pressure. According to Fig. 10, the MM process decreases the relative density of green compacts.

It is important to note that the densification behavior is influenced by the powder characteristics and the processing method. As the milling time increases, the green density of the compacts decreases due to the hardening effect of MM and change in particle size and morphology. The powder mechanically milled up to 10 h reached higher green densities than the powders mechanical milled for 5 h, due to the poor packing of the flattened powder. The higher applied pressure is required to activate higher plastic deformation capacity in flattened particles.

With increasing the milling time (up to 5 h), the powder morphology changed toward equiaxed, hence the relative density increased. At higher MM time, the compressibility behavior showed a decrease due to more increase in particles hardness. According to the compressibility curves, it is indicated that higher applied pressure is required to activate plastic deformation in the nanocomposite of higher MA time. Fig. 11 shows the fracture surface of for the Cu/4 vol% SiC compacts processed by MA for 0 h (simple mixture) and 25 h and pressed at $P=600$ MPa. Since the mixed composite has low hardness and high capability of deformation, it reaches a higher densification due to rearrangement and deformation of the particles, as can be seen in Fig. 11(a). For the 25 h milled composite, because of higher hardness of work hardened structure, the relative density of the compact is low, and the particles rearrangement is the main densification mechanism. From Fig. 11(b), no deformation sign is seen.

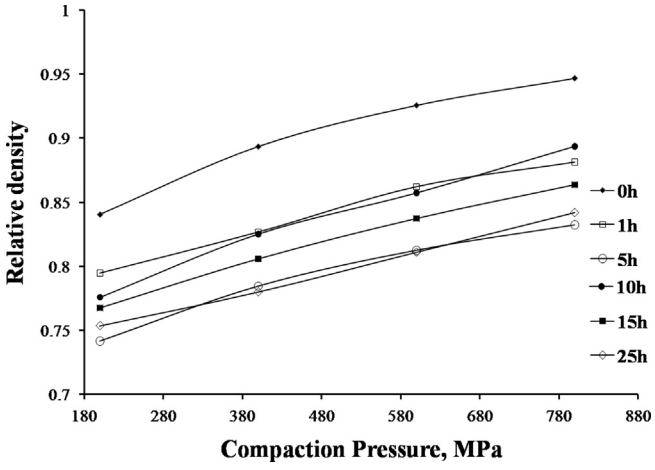

Fig. 10. The effect of compaction pressure on the relative density of Cu/4 vol% SiC mechanically milled for different times.

A classical way for the evaluation of the powder compressibility is the relationship between the density or porosity and the applied pressure [26–28]. Panelli and Ambrosio Filho [26] proposed the following equation:

$$\ln\left[\frac{1}{1-D}\right] = AP^{1/2} + B, \quad (1)$$

where D is the relative density of the compacted material, and P is the applied pressure. The authors showed that the parameter A (slope of the curve in Eq. (1)) is related to the plastic deformation capacity of the powder during the compaction process. High A values are obtained when soft metals such as Al or Cu are used; hard powders, like ceramics, show low A values. The parameter B (the intercept of the curve at zero pressure) expresses the density without pressure application, i.e. AD. However, due to the rearrangement mechanism at the beginning of compaction, B determined by Eq. (1) can be inaccurate [26].

The analysis of the compaction behavior by the compaction equations enables us to evaluate the effects of particle rearrangement at low pressures and plastic deformation at high pressures quantitatively. In this work, the Panelli–Ambrozio Filho compaction equation is used. The densification plots of Cu/4 vol% SiC powder after different MM time according to the Panelli–Ambrosio Filho equation are drawn in Fig. 12(a). As can be

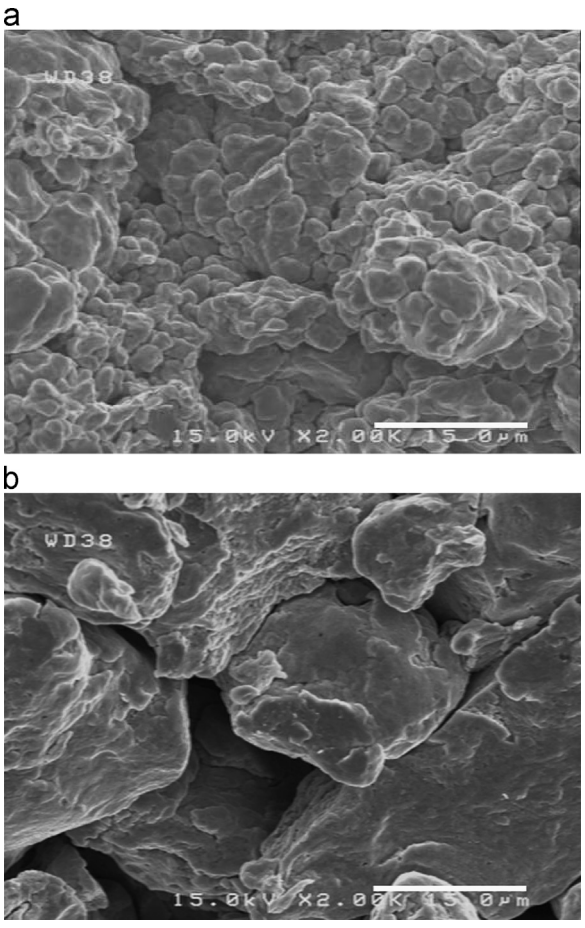

Fig. 11. Fracture surface of Cu/4 vol% SiC compacts pressed by $P=600$ MPa (scale bar: 15 µm): (a) as mixed powder and (b) MA processed for 25 h.

seen, the equation fits reasonably well to the experimental results ($R^2 > 0.989$). The variations of the A-value with MM time are shown in Fig. 12(b). The mixed composite powder shows the highest A-value, indicating the higher plastic deformation capacity. Generally, with increasing MM time the A-value decreases due to the increasing work hardening and high hardness. At the first stage of MM, despite the high deformation capability of the particles, the A-value is low due to the effect of the powder shape on the load transfer between two particles. The particles transmit the stress to their neighbor particles through the contact points between them. For the flattened particles, symmetrical opposite forces appears in the contact area (higher contact points than particles with irregular morphology) and decelerate compressive deformation of the particles. Low values for A due to MM during the first stage can be seen, due to the effect of particles morphology on the load transfer and the work-hardening rate [29].

Compressibility plots of the Cu reinforced with 0-6 vol% SiC powders processed by MM for 25 h fitted according to the Panelli-Ambrozio Filho equation are shown in Fig. 13(a) in order to investigate the effect of n-SiC on the deformation behavior of the nanocomposite powders. The Cu powder has higher A-value, indicating slightly higher plastic deformation capacity than the composites (Fig. 13(b)). The ratio of irregular to equiaxed particles in 2 h MM processed Cu is higher than that of the Cu reinforced with n-SiC. Relatively irregular morphology of the 25 h MM processed Cu particles induces the formation of asymmetrically opposite forces in the contact points between particles, which results in shear deformation and, consequently, cold-welding of the powder particles [29].The addition of the n-SiC particles in the Cu matrix decreases the A value, exhibiting lower plastic deformation due to the load partitioning effect. Symmetrical opposite forces in the contact points of the equiaxed nanocomposite particles promote only compressive deformation of particles. This shows that the addition of the n-SiC particles increases the densification of elemental Cu [15,16,22]. It is also observed that the plastic deformation capability of the nanocomposite powders was reduced as the milling of powder continued to 25 h and the effect of SiC particle is minor. The addition of the n-SiC particles to the Cu powder by MM improved the densification capacity. The A-values showed a slight change with nanoparticles addition, indicating that particle rearrangement at the initial stage of compaction accelerated the filling of voids between the matrix particles under the applied load. Therefore, the reduction of deformation capability after 25 h of MM made the rearrangement stage more dominant

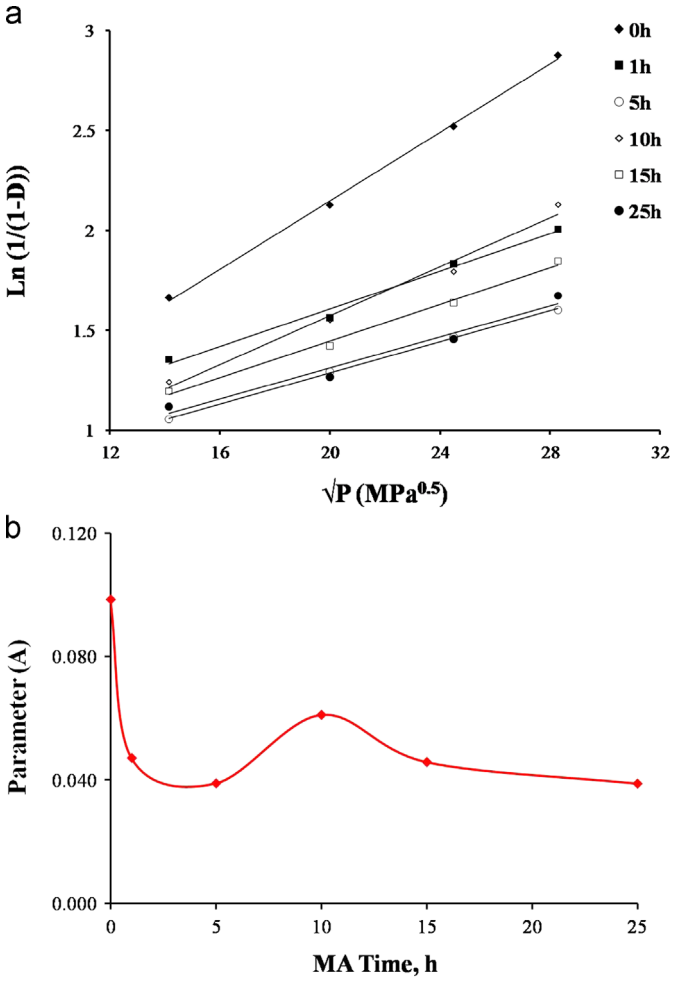

Fig. 12. (a) Experimental data of Cu/4 vol% SiC after high-energy mechanical milling for different times, fitted by the Panelli–Ambrozio Filho equation and (b) parameter A as a function of mechanical milling time.

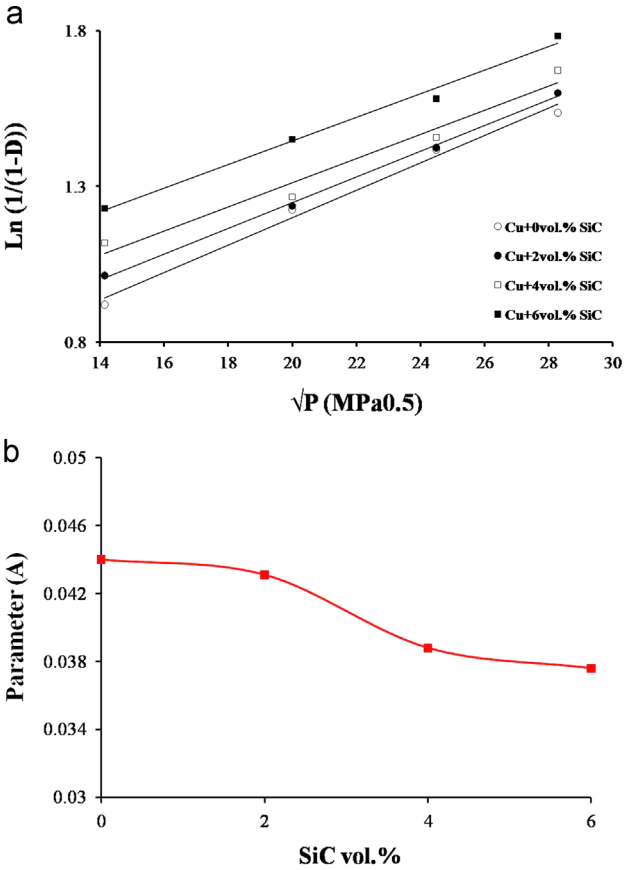

Fig. 13. (a) Experimental data of Cu/(0–6) vol% SiC after high-energy mechanical milling for 25 h, fitted by the Panelli–Ambrozio Filho equation and (b) parameter A.

mechanism of densification in the nanocomposite. Addition of SiC particles affects the densification of the nanocomposite by decreasing Hausner ratio, facilitating morphological change and reduction in particle size.

4. Conclusions

Cu reinforced with n-SiC particles was prepared with the MM process. The evolution of the microstructure during the MM process was investigated using XRD, SEM, TEM and microhardness test. Effects of MM time and SiC volume fraction on AD, TD, and compressibility of the powders were studied with the variation of the physical and mechanical properties of the powders. The conclusions can be summarized as follows:

(1) TD and AD were decreased continuously during the initial stage of milling; they reached a minimum value (up to 5 h) and then started to increase with prolonging the MM time, which is attributed to changes in the powder's morphology and hardness. HR increased with MM, which indicates that with increasing MM time the cohesivity of particles decreases.
(2) With increasing SiC content, TD, AD, and compressibility increase, while the Hausner ratio decreased. This is related to the change of the particle size and content of the powders with irregular morphology with increasing n-SiC. The addition of n-SiC to Cu powder results in a decrease in final particle size and the ratio of irregular to equiaxed particles content.
(3) The compressibility behavior of the powders were investigated in terms of particle rearrangement and plastic deformation mechanisms. The compaction data were best fitted to the Panelli–Ambrozio Filho equation in order to consider the effects of MM time and n-SiC content. Changes of powder morphology and hardness with increasing milling time affected the deformation capability of the powders according to *A*-values. It can be concluded that the major mechanism for densification at higher MM time is the particles rearrangement (higher hardness in comparison to the upper applied pressure during compaction). The n-SiC content influenced the compressibility of the nanocomposite powder by changing the rearrangement behavior with decreasing the Hausner ratio, decreasing particle size, and accelerating the morphological change.

Acknowledgments

This work was supported by the National Research Foundation of Korea(NRF) grant funded by the Korea government (MEST) (No. 2010-0026981).

References

[1] L. Zhu, H. Liu, B. Zhao, W. Shen, Hu, Microstructure and performance of electroformed Cu/nano-SiC composite, Mater. Des. 28 (2007) 1958–1962.
[2] N.B. Dhokey, R.K. Paretkar, Study of wear mechanisms in copper-based SiCp (20% by volume) reinforced composite, Wear 265 (2008) 117–133.
[3] S.G. Sapate, A. Uttarwar, R.C. Rathod, R.K. Paretkar, Analyzing dry sliding wear behaviour of copper matrix composites reinforced with pre-coated SiCp particles, Mater. Des. 30 (2009) 376–386.
[4] P. Buchner, D.L. Ützenkirchen-Hecht, H.H. Strehblow, J. Uhlenbusch, Production and characterization of nanosized Cu/O/SiC composite particles in a thermal r.f. plasma reactor, J. Mater. Sci. 34 (1999) 925–931.
[5] J. Boselli, P.D. Pitcher, P.J. Gregson, I. Sinclair, Numerical modelling of particle distribution effects on fatigue in Al–SiCp composites, Mater. Sci. Eng. A 300 (2001) 113–124.
[6] V.V. Bhanuprasad, R.B.V. Bhat, A.K. Kuruvilla, K.S. Prasad, A.B. Pandey, Y. Mahajan, P/M Processing of AI-SiC Composites, Int. J. Powder Metall. 27 (1991) 227.
[7] K. Hanada, Y. Murakoshi, H. Negishi, T. Sano, Microstructures and mechanical properties of Al-Li/SiCp composite produced by extrusion processing, J. Mater. Process. Technol. 63 (1997) 405.
[8] M.J. Tan, X. Zhang, Powder metal matrix composites: selection and processing, Mater. Sci. Eng. A 244 (1998) 80.
[9] Y.B. Liu, J.K.M. Kwok, S.C. Lim, L. Lu, M.O. Lai, Fabrication of Al–4.5Cu/15SiC composite: II. Mechanical properties, J. Mater. Process. Technol. 37 (1993) 441–451.
[10] L. Lu, M.O. Lai, C.W. Ng, Enhanced mechanical properties of an Al based metal matrix composite prepared using mechanical alloying, Mater. Sci. Eng. A 252 (1998) 203–211.
[11] R. Sankar, P. Singh, Synthesis of 7075 Al/SiC particulate composite powders by mechanical alloying, Mater. Lett. 36 (1998) 201–205.
[12] Z. Aslanoglu, Y. Karakas, M.L. Oveloglu, Switching performance of W–Ag electrical contacts fabricated by mechanical alloying, Int. J. Powder Metall. 36 (2000) 35–44.
[13] Naiqin Zhaoa, Philip Nashb, Xianjin Yang, The effect of mechanical alloying on SiC distribution and the properties of 6061 aluminum composite, J. Mater. Process. Technol. 170 (2005) 586–592.
[15] João B. Fogagnolo, Elisa M. Ruiz-Navas, Maria H. Robert, Jose´ M. Torralba, The effects of mechanical alloying on the compressibility of aluminium matrix composite powder, Mater. Sci. Eng. A 355 (2003) 50–55.
[16] Z. Razavi Hesabi, H.R. Hafizpour, A. Simchi, An investigation on the compressibility of aluminum/nano-alumina composite powder prepared by blending and mechanical milling, Mater. Sci. Eng. A 454–455 (2007) 89–98.
[17] R. Panelli, F. Ambrosio Filho, A study of a new phenological compacting equation, Powder Technol. 114 (2001) 255–261.
[18] K. Williamson, W.H. Hall, X-ray line broadening from filed aluminium and wolfram, Acta Metall. 1 (1953) 22–31.
[19] C. Suryanarayana, Mechanical alloying and milling, Prog. Mater. Sci. 46 (2001) 1–184.
[20] M. Adamiak, Mechanical alloying for fabrication of aluminium matrix composite powders with Ti–Al intermetallics reinforcement, J. Achiev. Mater. Manuf. Eng. 31 (2008) 191–196.
[21] K. Gan, M. Gu, The compressibility of Cu/SiC powder prepared by high-energy ball milling, J. Mater. Process. Technol. 199 (2008) 173–177.
[22] J.B. Fogagnolo, F. Velasco, M.H. Robert, J.M. Torralba, Effect of mechanical alloying on the morphology, microstructure and properties of aluminium matrix composite powders, Mater. Sci. Eng. A 342 (2003) 131–143.
[23] A. Alizadeh, E. Taheri-Nassaj, H.R. Baharvandi, Preparation and investigation of Al–4 wt% B4C nanocomposite powders using mechanical milling, Bull. Mater. Sci. 34 (2011) 1039–1048.
[24] Alisa Vasilenko, Sara Koynov, Benjamin J. Glasser, Fernando J. Muzzio, Role of consolidation state in the measurement of bulk density and cohesion, Powder Technol. 239, (2013), 366–373.
[25] J Vonazountas, T.J. Davies, Advances in P/M & Particulate Materials, 2nd ed., Metal Powder Industries Federation, New Jersey, USA89–113.
[26] R. Panelli, F.A. Filho, A study of a new phenomenological compacting equation, Powder Technol. 114 (2001) 255–261.

[27] E. Hryha, E. Dudrová, S. Bengtsson, Influence of powder properties on compressibility of prealloyed atomised powders, Powder Metall. 51 (2008) 340–342.

[28] P.J. Denny, Compaction equations: a comparison of the Heckel and Kawakita equations, Powder Technol. 127 (2002) 162–172.

[29] W. Schatt, K. Wieters, Powder Metallurgy/Processing and Materials, European Powder Metallurgy, Association (EPMA), Shrewsbury, UK 5–44.